Research Article

Zhuo Li, Kun Zhang*, Yan Song*, Xiaoxue Liu*, Zhenxue Jiang*, Shu Jiang*, Ming Wen, Yizhou Huang, Chengzao Jia, Weiwei Liu, Xin Wang, Xin Li, Zhiyuan Chen, Ling Tang, Pengfei Wang, Tianlin Liu, and Xuelian Xie

Source Analysis of Silicon and Uranium in uranium-rich shale in the Xiuwu Basin, Southern China

https://doi.org/10.1515/geo-2019-0008
Received Dec 17, 2018; accepted Feb 22, 2019

Abstract: Uranium deposits are crucial resources for the development of the nuclear energy. Among known sources of uranium, the uranium-rich shales have recently obtained significance. In this paper, the Lower Cambrian Wangyinpu Formation shale in the Xiuwu Basin, southern China, has been studied using a combination of techniques including element analysis (Al, Fe, and Mn), δ^{30}Si silicon isotopic analysis, δ^{18}O oxygen isotopic analysis, study of core samples. It has been observed that significant hydrothermal activity occurred in the Xiuwu Basin during the Early Cambrian period. The results show that 20%–40% of the silicon in most of the sections of the Lower Cambrian Wangyinpu Formation were inherited from the hydrothermal fluids, with temperatures ranging between 75°C and 102°C. It is concluded that more than 90% of the uranium in most of the sections of the Lower Cambrian Wangyinpu shale was derived from submarine hydrothermal fluids, while less than 10% from the terrigenous detritus. The enrichment of uranium in the basin was observed in the Middle-Upper part of the Wangyinpu Formation and the geological resources estimated to a tune of ~4.9×10^3 t. In this paper, we proposed a model for silicon and uranium enrichment in the Lower Cambrian shale controlled by hydrothermal activity in the Xiuwu Basin. This model also provides a scientific rationale for uranium further exploration and exploitation of the uranium resource.

Keywords: Source of uranium element; Submarine hydrothermal activity; Hydrothermal silicon; Hydrothermal uranium; Uranium resources

***Corresponding Author: Kun Zhang:** State Key Laboratory of Petroleum Resources and Prospecting, China University of Petroleum, Beijing 102249, China; Unconventional Natural Gas Institute, China University of Petroleum, Beijing 102249, China; Unconventional Petroleum Collaborative Innovation Center, China University of Petroleum, Beijing 102249, China; Research Institute of Petroleum Exploration and Development, Beijing 100083, China; Key Laboratory of Tectonics and Petroleum Resources of Ministry of Education, Faculty of Earth Resources, China University of Geosciences, Wuhan 430074, China; Email: shandongzhangkun@126.com

***Corresponding Author: Yan Song:** State Key Laboratory of Petroleum Resources and Prospecting, China University of Petroleum, Beijing 102249, China; Unconventional Natural Gas Institute, China University of Petroleum, Beijing 102249, China; Research Institute of Petroleum Exploration and Development, Beijing 100083, China; Email: sya@petrochina.com.cn

***Corresponding Author: Xiaoxue Liu:** State Key Laboratory of Petroleum Resources and Prospecting, China University of Petroleum, Beijing 102249, China; Unconventional Natural Gas Institute, China University of Petroleum, Beijing 102249, China; Email: Iris_1314_Iris@163.com

***Corresponding Author: Zhenxue Jiang:** State Key Laboratory of Petroleum Resources and Prospecting, China University of Petroleum, Beijing 102249, China; Unconventional Natural Gas Institute, China University of Petroleum, Beijing 102249, China; Email: zhenxuejiangedu@126.com

***Corresponding Author: Shu Jiang:** Key Laboratory of Tectonics and Petroleum Resources of Ministry of Education, Faculty of Earth Resources, China University of Geosciences, Wuhan 430074, China; Research Institute of Unconventional Oil & Gas and Renewable Energy, China University of Petroleum (East China),Qingdao 266580, China; Energy and Geoscience Institute, University of Utah, Salt Lake City, Utah 84108, United States; Email: sjiang@egi.utah.edu

Zhuo Li, Ming Wen, Yizhou Huang, Xin Wang, Tianlin Liu: State Key Laboratory of Petroleum Resources and Prospecting, China University of Petroleum, Beijing 102249, China; Unconventional Natural Gas Institute, China University of Petroleum, Beijing 102249, China

Chengzao Jia: Research Institute of Petroleum Exploration and Development, Beijing 100083, China

Weiwei Liu: Jiangxi Provincial Natural Gas Company, Ltd., Nanchang 330000, China

Xin Li, Zhiyuan Chen, Ling Tang: State Key Laboratory of Petroleum Resources and Prospecting, China University of Petroleum, Beijing 102249, China; Unconventional Natural Gas Institute, China University of Petroleum, Beijing 102249, China; Unconventional Petroleum Collaborative Innovation Center, China University of Petroleum, Beijing 102249, China

1 Introduction

Uranium deposits are important strategic and energy mineral resources as well as basic raw materials for the nuclear industry [1–5]. Due to increasing domestic demand, China needs to generate more power to propel its economic development. Nuclear power is favored because of it is clean and efficient. In 2007, China proposed the goal of building 40 million kilowatts of nuclear power by 2020 and maintaining 18 million kilowatts of nuclear power under construction. According to estimates of the speed and scale of nuclear power development, a considerable amount of uranium resources is needed to meet future development goals. China has abundant uranium resources scattered in many types of deposits including granite-, volcanic-, sandstone-, and shale-hosted deposits [6, 7]. The shale-type uranium deposit is one of the earliest types of industrial uranium deposits that were discovered. In 1893, the world's first shale-type uranium deposit was discovered in Sweden. After 1940s, shale-type uranium emerged as an important type of uranium deposit for the mining industry during the peak of uranium exploration [8, 9]. Subsequently, several shale-type uranium deposits were discovered in Sweden, the United States, Norway, Germany, Russia, Kazakhstan, Uzbekistan, Germany, South Korea and China [10].

Uranium-rich shale is rich in U and Si. There is abundant uranium in the shales of the Lower Cambrian Wangyinpu Formation in Xiuwu Basin; however, determining source of this uranium is still not known [11–13]. Previous studies were focused on understanding the source of silicon, in this paper we are constraining the source of uranium in shale. It is believed that some special sedimentary structures and minerals can be formed by seafloor hydrothermal activity [14–17]. For special sedimentary structures, there are scour surface, columnar structures, vein structures, contraction-like structures, horizontal laminated bed structures and nodules. In addition, special minerals mainly refer to hydrothermal silica and uranium. Holdaway and Clayton (1982) used excess siliceous minerals (*i.e.*, siliceous minerals beyond the normal terrigenous clastic sources) and proposed a method to quantitatively calculate excess siliceous mineral [18]. Wedepohl (1971), Adachi *et al.* (1986) and Yamamoto (1987) proposed a method using the Al-Fe-Mn ternary plot to determine hydrothermal versus biogenic origin of silicate minerals [19–21]. Whereas, Bostrom *et al.* (1973) and Douthitt *et al.* (1982) proposed a method of determining origin of siliceous mineral using silicon isotopes [22, 23]. Furthermore, Savin *et al.* (1970) and Knauthand Epstein (1976) proposed a method for calculating hydrothermal temperatures suing oxygen isotopes [24, 25]; Taylor and McLennan(1985) and Algeo *et al.* (2011) devised a method for calculating the elemental composition from non-terrestrial debris based on post-Archean Australian shale (PAAS) standard values [26, 27]. In this paper we assess the relationship between silicon and uranium and characterize the source of uranium in the Lower Cambrian shale of the Xiuwu Basin. We further propose the enrichment model for silicon element and uranium in the Lower Cambrian shale and its utility for exploration and mining of uranium in the Xiuwu Basin.

2 Geological settings

2.1 Sedimentary and stratigraphic characteristics

In the early period of the Early Cambrian, sedimentary environments of the Yangtze Plate from northwest to southeast were ancient land, shallow shelf, deep shelf, continental slope, and oceanic basin (Figure 1); whereas those from the Cathaysian Plate from northwest to southeast were ocean basin, continental slope, deep shelf, shallow shelf, and ancient land [28, 29]. The environment at the junction of the two plates was an ocean, with deep water gradually shallowing to both sides of the ancient land and the Xiuwu Basin was in a deep anoxic reducing environment [28, 29].

One of the goals of this paper is to describe a set of strata that was widely deposited on the Yangtze Plate and the Cathaysian Plate during the Early Cambrian. Due to its vast distribution, it has been given different names in different regions, for *e.g.* in the Lower Yangtze region, it is known as Wangyinpu Formation. It is characterized by a set of black-dark gray organic-rich shale deposited in the Early Cambrian, which is one of the key exploration targets for shale gas in China.

2.2 Tectonic characteristics

During the Sinian period, the Xiuwu Basin was an intracratonic basin. A marine regression at the end of the Sinian

Pengfei Wang: Geoscience Documentation Center. CGS, Beijing 100083, China
Xuelian Xie: Guangzhou Marine Geological survey, Guangzhou 510760, China
Zhuo Li, Kun Zhang, Ming Wen and Yizhou Huang contributed equally to this work

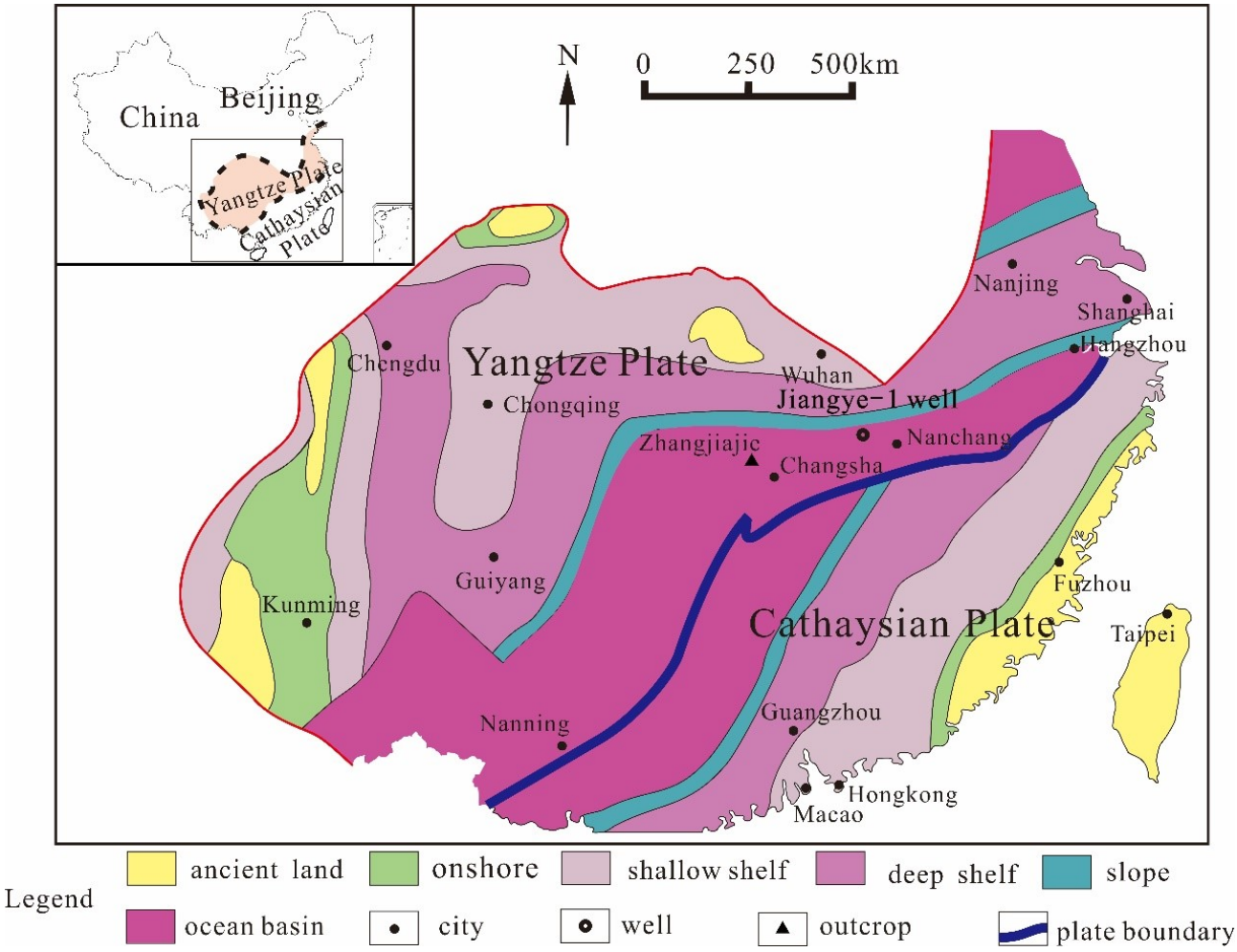

Figure 1: The sedimentary characteristics of the Yangtze Plate and the Cathaysian Plate during the Early Cambrian in South China. The hydrothermal activity in the Early Cambrian came from the junction of the Yangtze Plate and the Cathaysian Plate. And the Jiangye-1 well in Xiuwu Basin was close to the junction of the plate, so the Lower Cambrian shale in Jiangye-1 well was affected by the hydrothermal activity during sedimentation. Modified after references [28 and 29].

period formed the Piyuancun Formation, which was dominated by siliceous dolomite. Subsequently, a large-scale transgression occurred in the Early Cambrian, forming the Wangyinpu Formation black shale, which was rich in organic matter and had a thickness of 45–60 m. After that, the sea level gradually became shallower, and the sedimentary environment of the Guanyintang Formation transitioned into a shallow water shelf [30]. The sedimentary system shifted from the Early Cambrian clastic sedimentary system into the Middle-Late Cambrian carbonate sedimentary system before transitioning back into a clastic sedimentary system in the Early Middle Ordovician period [31]. Due to plate collision in the Late Ordovician-Early Silurian, the study area was squeezed to form a deep-water environment. During the Middle Silurian period, the water body gradually became shallower, and the study area was uplifted to the ancient land surface in the Late Silurian period [32–37].

3 Samples, experiments and data sources

3.1 Mineral composition analysis

In this paper, 20 core samples were taken from the Lower Cambrian Wangyinpu Formation in Jiangye-1 well, and the mineral composition was analyzed by ZJ207 Bruker D8 advance X-ray diffraction instrument.

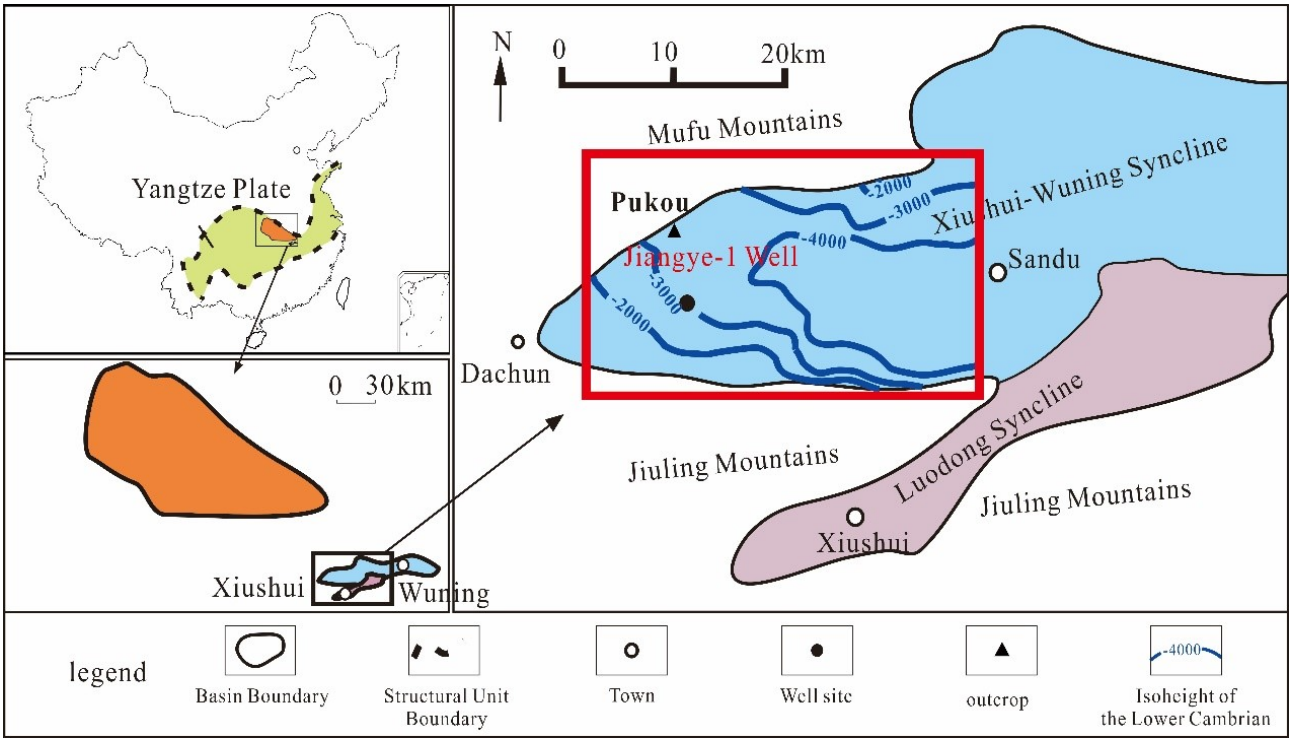

Figure 2: The Xiuwu Basin is located in the Lower Yangtze area on the southeastern side of the Jianghan Basin. It consists of the Xiushui-Wu Ning and Luodong synclines. The study area is located on the west side of the Xiushui-Wuning syncline, in which the Jiangye-1 well is drilled.

3.2 Elemental log data

This paper included elemental log data (U, Si, Al, and Th) from two wells provided by the Schlumberger Corp with a data point every 0.125 m of depth.

3.3 Elemental analysis

In this study, 87 core samples of the Cambrian Wangyinpu Formation from the Jiangye-1 well were taken approximately 0.5 m–1 m apart. The elemental analysis of core samples from the Jiangye-1 well was carried out by X-ray fluorescence spectrometry (Axios-MAX), and the mass percentage of Al, Fe and Mn was obtained.

3.4 Analysis of silicon and oxygen isotopes

Three core samples from the Lower Cambrian Wangyinpu Formation in Jiangye-1 well were selected for the measurement of silicon and oxygen isotopes using the MAT-251EM mass spectrometer in Nanjing University. The number and depth of samples are shown in Table 1. The silicon isotope analysis method is the SiF_4 method, in which the samples were crushed to 200 mesh, calcined, their organic matter was removed, and then they were soaked in HCl to remove siderite and other sulfides. The purified samples (SiO_2) were reacted with BrF_5 at a constant temperature of 550°C to form SiF_4 gas. The purified SiF_4 gas obtained through the liquid N_2 trap purification process was measured by mass spectrometry. Based on international standard NBS-28, the analytical error limitation was ±0.1%ffl. The method of oxygen isotope analysis was also based on the BrF_4 method measured by mass spectrometry using the international standard VSMOW, the analytical error limitation was ±0.2%ffl. In addition to the silicon and oxygen isotope measurements of the three samples carried out in this study, the silicon isotope and oxygen isotope data of the Zhangjiajie profile of Hunan Province having same sedimentary environment were used for comparison.[38]

Table 1: The number, depth, and formation of core sample of silicon isotope and oxygen isotope experiments in Jiangye-1 well. See Figure 1 and 2 for the well location.

Number	Well	Depth (m)	Formation
1	Jiangye1	2629	Wangyinpu
2	Jiangye1	2645	Wangyinpu
3	Jiangye1	2663	Wangyinpu

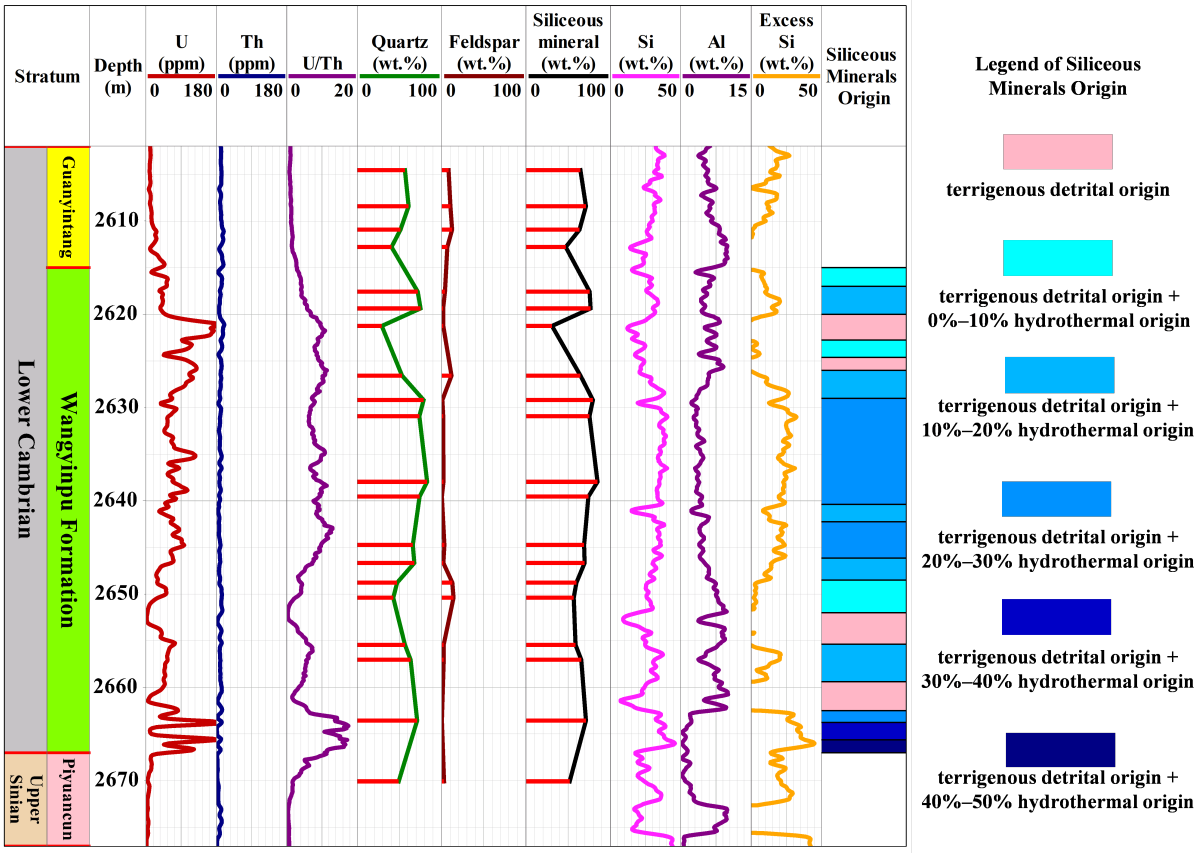

Figure 3: Determination of redox environment and calculation results of source of the excess siliceous mineral in Wangyinpu Formation of Cambrian during sedimentary period. In layers where excess siliceous mineral is present, the excess siliceous mineral in half of the layers is between 20% and 30%, and the excess siliceous mineral in some layers is between 30% and 40%, even reaching 40% to 50%. See Figure 1 for the well location.

3.5 Cores and field profile observation

In this study, core samples (total 72m thick) in the Lower Cambrian Wangyinpu Formation along with its overlying and underlying strata were logged in detail. Additionally, the Pukou profile (Lower Cambrian outcrop) in the northern side of the Xiuwu Basin was also recorded in detail.

4 Results and Discussion

4.1 Redox environment during the sedimentary period of the Lower Cambrian Wangyinpu Formation in Jiangye-1 well

Various methods have been used to decipher sedimentary environments including geochemical proxies. Among these, U/Th ratio had been effectively used to characterize the sedimentary redox conditions [19–21]. Generally speaking, U/Th > 1.25 represents anoxic environment, U/Th ratio between 0.75 and 1.25 represents dysoxic environment, and U/Th < 0.75 represents oxidizing environment. As can be seen from Figure 3, the redox index (U/Th ratio) of the Lower Cambrian Wangyinpu Formation in Jiangye-1 well during the shale deposition period is very high (4-18), which indicates that a strong anoxic environment prevailed at the time of deposition.

4.2 Source analysis of silicon in the Lower Cambrian shale

Using Si and Al log data from Jiangye-1 well, the excess siliceous mineral from a non-terrigenous clastic source was calculated, and the excess silicate minerals were identified with an Al-Fe-Mn ternary plot. Further, silicon isotope analyses were used to estimate the hydrothermal activity in the deposition of shale and temperature of the hy-

drothermal fluid was calculated using oxygen isotopes, as discussed below.

4.2.1 An Al-Fe-Mn ternary plot to determine the source of silicate minerals

In shale, the silicon is concentrated in silicate minerals, namely, quartz and feldspar, more so in the form of pure quartz (SiO_2).The common sources of silicon are: terrestrial detrital deposits, hydrothermal silicon, and biogenic silicon [22, 39, 40]. During the hydrothermal activity, seawater reaches deeper parts of seabed through fissures and faults and exchange their chemical components with the crustal rocks. The infiltrated seawater gets heated by the heat supplied by underground magma chambers or extruded basalts, and manifest them in the form of submarine hot springs. The trace elements including most metallic elements in the hydrothermal are therefore quite different from those present in the ordinary seawater [41, 42].

Excess silicates (abbreviated as Si_{ex}) refers to those, excluding normal terrigenous clastic deposits. These were calculated by using following formula:

$$Si_{ex} = Si_s - \left[(Si/Al)_{bg} \times Al_s\right]$$

Si_s refers to silicon in the sample, Al_s is the aluminum element in the sample, and $(Si/Al)_{bg}$ is 3.11, which is based on the average composition of the shale [18]. According to Si and Al log curves provided by Schlumberger Corp, this formula has been used to calculate the excess siliceous mineral from the Jiangye-1 well in the Lower Cambrian Wangyinpu Formation, and the results are shown in Figure 3. It was observed that there is excess silica in most layers of the Wangyinpu Formation. In the layers where excess silica is present, about half of the layers have Si_{ex} between 20% and 30%, and in some layers, Si_{ex} is between 30% and 40%, occasionally reaching 40% to 50%.

Wedepohl (1971), Adachi *et al.* (1986) and Yamamoto (1987) proposed a method using the Al-Fe-Mn ternary plot to determine whether the excess silica is derived from hydrothermal or biogenic sources [19–21]. As shown in Figure 4, the data fall within the hydrothermal field of the ternary plot, indicating that the excess silica is hydrothermal origin.

4.2.2 The silicon and oxygen isotopes

The δ^{30}Si value in siliceous rocks has regular changes in different sedimentary environments. Therefore, the δ^{30}Si value can be considered as an important index for judging the origin of silica and its depositional environment. Generally, the δ^{30}Si value of quartz from hydrothermal source is very small, ranging from –1.5‰ to +0.8‰; the δ^{30}Si value of authigenic quartz in groundwater ranges from +1.1‰ to +1.4‰; the δ^{30}Si value of quartz in metasomatic siliceous rock is higher, ranging from +2.4‰ to +3.4‰ [22, 23, 43].

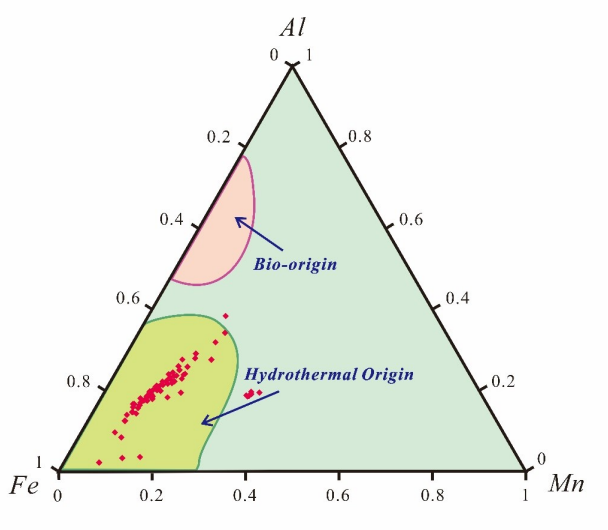

Figure 4: Through the Al-Fe-Mn ternary plot analysis, it is found that siliceous mineral from the Lower Cambrian Wangyinpu Formation in the Jiangye-1 well contain excess siliceous mineral, which is derived from hydrothermal origin. See Figure 1 for the well location. I is the bio-origin, and II is the hydrothermal origin.

In this study, the δ^{30}Si values of the three core samples from the Lower Cambrian Wangyinpu Formation shale in the Xiuwu Basin, Jiangxi Province are +0.1‰, –0.3‰, –0.6‰ respectively, as shown in Table 2 (the samples numbered from 1 to 3). Previous δ^{30}Si analysis of the Lower Cambrian shale in the Zhangjiajie, Hunan Province, showed that values were –0.3‰, –0.4‰, –0.5‰ respectively [38], as shown in Table 2 (The samples numbered from 4 to 6). The δ^{30}Si values of the six samples are all in the range of –1.5‰ – +0.8‰, which indicates that in the Early Cambrian, the sedimentary environment was an oceanic basin affected by hydrothermal activity between the Yangtze Plate and the Cathaysian Plate.

The oxygen isotope composition of shale is an important index for studying the genesis of silica [24, 25]. Quartz with different origins has different δ^{18}O values. The δ^{18}O value of igneous quartz ranges from 8.3‰ to 11.2‰, with an average of 9‰; the δ^{18}O value of metamorphic quartz ranges from 11.2‰ to 16.4‰, with an average of 13‰–14‰; and the δ^{18}O value of hydrothermal quartz ranges from 12.2‰ to 23.6‰ [24, 25]. For modern beach sand quartz, δ^{18}O value ranges from 10.3‰ to 12.5‰,

Table 2: Silicon and oxygen isotope composition of the Lower Cambrian shale and temperature of the sedimentary environment calculated from empirical formulas. The δ^{30}Si and δ^{18}O values of No. 1-3 are from the Lower Cambrian shale in Jiangye-1 of Xiuwu Basin, Jiangxi Province. The δ^{30}Si and δ^{18}O values of No. 4-6 are from the Lower Cambrian shale of Zhangjiajie, Hunan Province [38].

Sample Number	δ^{30}Si (‰)	δ^{18}O (‰)	The temperature calculated according to formula (1) °C	The temperature calculated according to formula (2) °C
1	0.1	22.2	75	77
2	−0.3	18.6	102	92
3	−0.6	21	83	82
4	−0.4	19.1	98	90
5	−0.5	21.6	79	80
6	−0.3	20.9	84	83

with an average of 12‰. According to the experimental results, the δ^{18}O values of the three core samples from the Lower Cambrian Wangyinpu Shale in the Xiuwu Basin, Jiangxi Province, are +18.6‰, +21‰, +22.2‰ respectively (Table 2). Jiang and Li (2005) performed a δ^{18}O analysis of the Lower Cambrian shale in Zhangjiajie, Hunan Province, the sedimentary environment of which was also an ocean basin in the Early Cambrian period, with values of +19.1‰, +20.9‰, and +21.6‰ (Table 2) [38]. The results show that the oxygen isotope of the target layer in the study area is significantly different from that of igneous quartz, metamorphic quartz, and modern beach sand quartz and is distributed within the range of δ^{18}O value of hydrothermal quartz, reiterating hydrothermal origin for excess silica.

The oxygen isotope composition of silicate rocks can be used to calculate the temperature of the ancient ocean [25]. The method for calculation of temperature is shown in the following two empirical formulas:

$$\delta^{18}\mathrm{O\,(Shale)} - \delta^{18}\mathrm{O\,(Seawater)} = 3.09 \times 10^6/\mathrm{T}^2 - 3.29 \quad (1)$$

$$\mathrm{t}/^{\circ}\mathrm{C} = 5.0 - 4.1 \times [\delta^{18}\mathrm{O\,(Shale)} - \delta^{18}\mathrm{O\,(Seawater)} - 40] \quad (2)$$

δ^{18}O (shale) is the oxygen isotope composition of shale; δ^{18}O (seawater) is the oxygen isotope composition of the sedimentary medium (seawater). In formula (1), T is the thermodynamic temperature. In the above two formulas, the oxygen isotope composition of the sedimentary medium is unknown, but previous studies have shown that the oxygen isotope composition of seawater does not change much from ancient to modern. Therefore, it is assumed that the oxygen isotopic composition of ancient seawater is same as that of modern seawater, 0‰ [25, 44].

Based on above assumptions, the samples from the target layer in the study area (the samples numbered from 1 to 3) were used to calculate temperature with formula (1). The temperature of hydrothermal fluids in the Early Cambrian ancient sea in the study area (the samples numbered from 1 to 3) ranged from 75°C to 102°C. The samples from Zhangjiajie, Hunan Province, within the same sedimentary environment (the samples numbered from 4 to 6) revealed a temperature of 79°C to 98°C for the hydrothermal fluids in the Early Cambrian ancient sea. According to formula (2), the temperature of hydrothermal fluids in the Early Cambrian ancient sea in the study area (samples 1-3) varied from 77°C to 92°C. The samples from Zhangjiajie, Hunan Province, within the same sedimentary environment (samples 4-6) revealed temperatures of the hydrothermal fluids in the Early Cambrian ancient sea varied from 80°Cto 90°C. Since the samples used in this experiment can be of uncertain origin, there could be some contribution of excess silica contributed by the terrigenous deposits in addition to hydrothermal silica. However, it is clear that the temperature of ancient seawater was still much higher. Bearing *et al.* (2018) recently proposed that the seawater temperature near the equator during the Early Cambrian was 35°C–45°C [44]. According oxygen isotope data, the calculated temperature of the seawater in the Lower Cambrian ocean in the study area (75°C to 102°C) was much higher than that near the equator (35°C–45°C), indicating that the ocean between the Yangtze Plate and the Cathaysian Plate in the Early Cambrian was greatly affected by exhalation of hydrothermal solutions.

4.2.3 Special sedimentary structures

In the deep sea where the sedimentary environment is relatively low-energy, shale with horizontal bedding and massive bedding will develop [45–48]. If hydrothermal activity exists in the seabed, due to the fast flow rate and large flow volume, it will be easy to form special sedimentary struc-

tures in the relatively soft seabed sediments, thus providing a basis for identifying hydrothermal activity.

(1) Scour surface

Scour surface refers to the uneven sedimentary surface caused by scouring the underlying sediments because of increased water flow rate, which indicates that there is a strong scour process after the underlying strata deposition [17]. The top of the consolidated and semi-consolidated deep seabed sediments will become an uneven erosional surface due to the scour of hydrothermal activity. Above the scour surface, when the sediments get deposited again, fragments and gravel from the underlying strata, which are washed down are often deposited in the gullies and grooves formed by scour (Figure 5A). The scour surface is relatively smooth and undulating, which indicates that it formed by submarine hydrothermal fluids scouring.

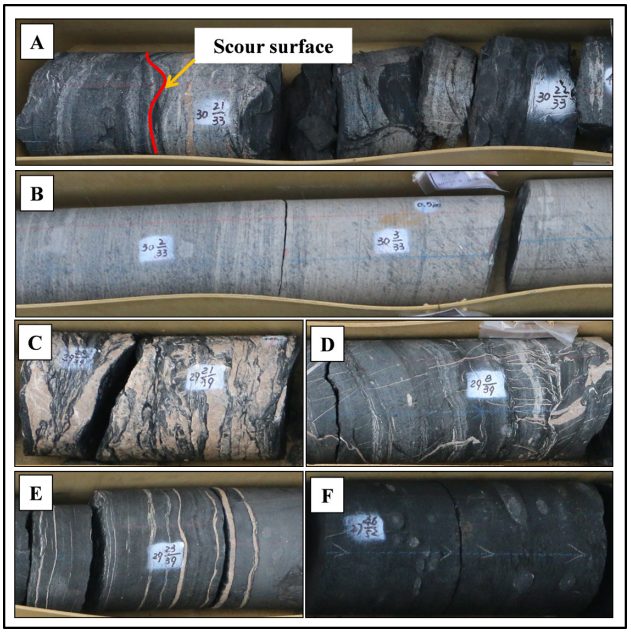

Figure 5: Sedimentary structures in shale in the Lower Cambrian Wangyinpu Formation from the Jiangye-1 well. A: Scour surface, B: Columnar structures; C: Vein structures; D: Contraction-like structures; E: Horizontal laminated bed structures; F: Nodules. See Figure 1 for the well location.

(2) Columnar structures

At the bottom of the Lower Cambrian Wangyinpu Formation, in addition to the development of the scour surface structures, a large number of columnar barite bodies were formed (Figure 5B). The columnar body is composed of barite that is usually ~1 m in length and ~15 cm in diameter. The formation of columnar barite might be caused by quick exhalation of high density $BaSO_4$. Due to the high density and quick exhalation, it crystallized without mixing with seawater.

(3) Vein structures

A large number of veined barite bodies were found in the Lower Cambrian Wangyinpu shale. This is because when the seabed sediments had not been consolidated, they were invaded by hydrothermal fluids rich in $BaSO_4$, causing strong deformation of the shale (Figure 5C). These structures were formed because the cracks were filled with barite.

(4) Contraction-like structures

Some dry crack-like structures were often found on carbonaceous shale from the barite ore floor (Figure 5D). The cracks were filled with carbonaceous shale containing barite that may be formed by hydrothermal fluids filling cracks in the underlying bed.

(5) Horizontal laminated bed structures

Horizontal laminated bed structures of organic shale and barite layers can be formed in the shale (Figure 5E). The sedimentary structures were well developed in hydrothermal sedimentary rocks, particularly in the late stage of hydrothermal venting-flowing process or at the periphery of the vents.

(6) Nodules

Barite nodules were products formed by a small amount of exhalative material at the end of the exhalation of fluids rich in $BaSO_4$. Barite nodules generally were ~5 cm in diameter and ~2 cm in height and were densely packed (Figure 5F).

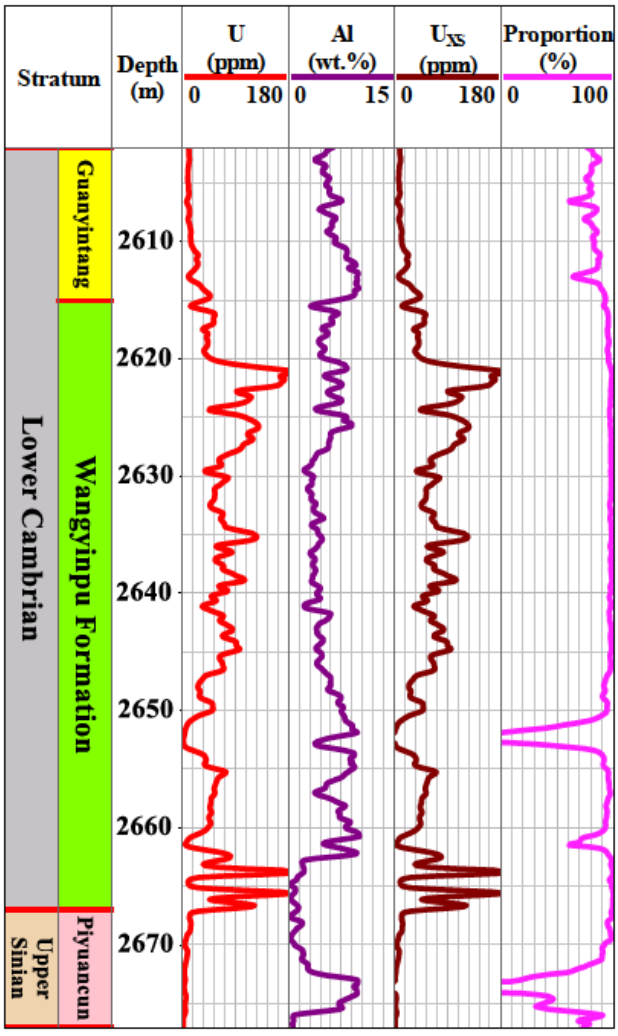

Figure 6: Results of excess uranium U_{XS} (uranium element from non-terrigenous detrital origin) calculations in the Cambrian Wangyinpu Formation in downhole Jiangye-1 See Figure 1 for the well location.

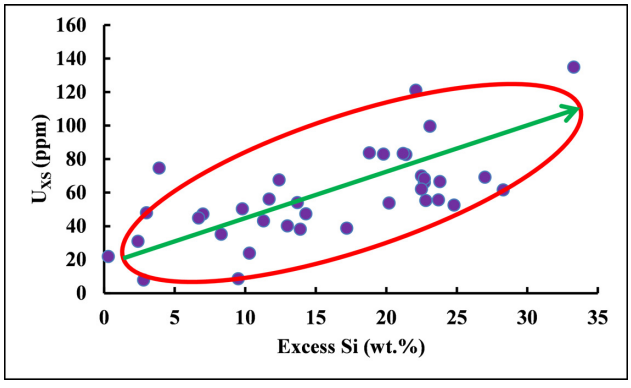

Figure 7: Correlation analysis of excess uranium (U_{XS}) and excess siliceous material in the Lower Cambrian Wangyinpu Formation from Jiangye-1 well. See Figure 1 for the well location.

The Lower Cambrian Wangyinpu Formation displayed a variety of sedimentary structures: scour surface, columnar structures, vein structures, contraction-like structures, horizontal laminated bed structures, and nodules, and all constituted a typical structural assemblage resulting from hydrothermal exhalation, indicating the process of submarine exhalation from beginning to end.

From above analysis, hydrothermal activity was relatively developed at the junction of the Early Cambrian Cathaysian Plate and the Yangtze Plate due to extension between the two plates. As a result, silicon in shale was not only derived from terrestrial detritus, but also contained deep crustal materials produced by the hydrothermal activity.

4.3 Analysis of uranium source

In seawater, the concentration of uranium was very less. Similar to silicon, uranium in oceanic water mainly also comes from two sources: terrigenous and non-terrigenous source. Uranium from non-terrigenous source is called excess uranium (U_{XS}), and its content can be calculated by the total content of uranium (Us) minus the estimated content [$Al_s(U/Al)_{PAAS}$] derived from terrigenous detritus. The formula is expressed as given below:

$$U_{XS} = U_s - Al_s(U/Al)_{PAAS}$$

Where, U_s – total content of U in shale sample, Al_s–total content of Al in the shale sample. The PAAS is the chosen standard shale in Australia [26]. The $(U/Al)_{PAAS}$ is the ratio of the two elements in the shale, specifically, 3.67×10^{-5}, and the U_{XS} is the excess value of uranium. If U_{XS} is positive, it indicates that there is a uranium component of non-terrigenous origin. If U_{XS} is negative, it indicates that the uranium in the sample is from terrigenous detritus. The U_{XS} value for current samples is shown in Figure 6. The results indicate that there is uranium of non-terrigenous origin in most layers of the Wangyinpu Shale, and in the layers containing non-terrigenous uranium, the proportion of uranium from a non-terrigenous source is greater than 90%. Aluminum was related to terrestrial debris, but the uranium from non-hydrothermal origin was also related to other factors. Therefore there was an error in the calculation of formula.

Hydrothermal activity can introduce various elements into sedimentary materials, including metals such as Na, Mg, Ca, Fe, Mn, Zn, Cu, and K; radioactive elements such as U and Th; and non-metallic elements such as Si, S, and P [49]. The organic matter has great adsorption capacity in adsorbing uranium from seawater, which catalyzes ura-

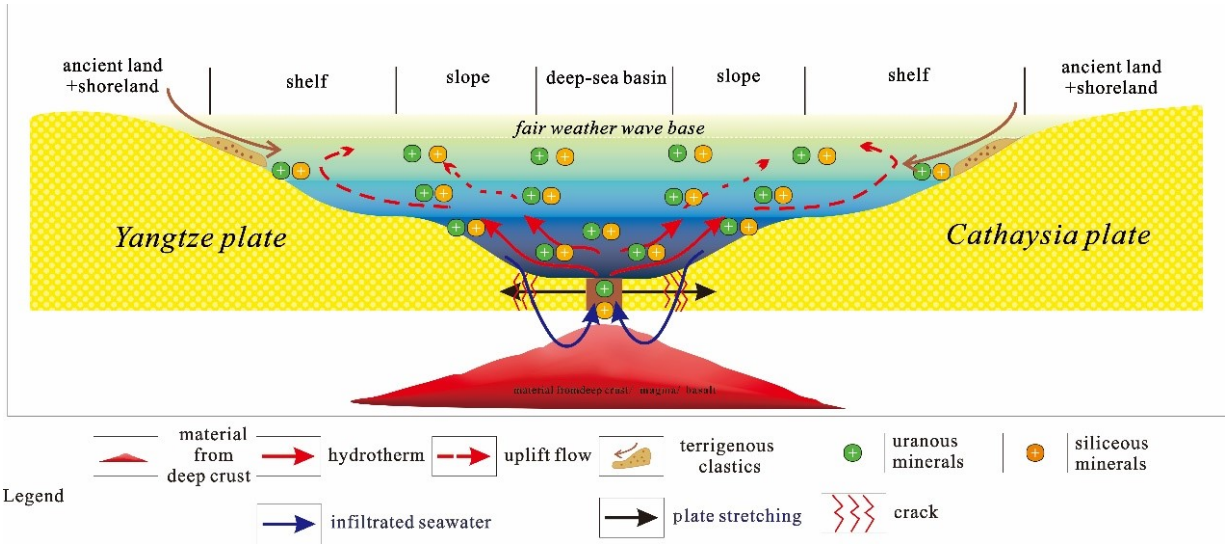

Figure 8: The model of the source of silicon element and uranium element in the Xiuwu Basin during Early Cambrian. 20%–40% of silicon comes from seafloor hydrothermal fluids, the rest comes from terrigenous detritus; more than 90% of uranium comes from seafloor hydrothermal fluids, less than 10% from terrigenous detritus.

nium deposition. A correlation between excess uranium and excess silica in the Wangyinpu shale is shown in Figure 7, which shows a significant positive correlation. It appears that since the excess silica was derived from hydrothermal fluids, excess uranium might also be derived from the hydrothermal fluids. By this analogy, more than 90% of the uranium in most of the Wangyinpu shale was derived from the hydrothermal activity in Xiuwu Basin during the Early Cambrian period, leaving less than 10% U contribution from the terrigenous detritus.

Figure 6 shows the uranium is concentrated in the Middle-Upper part of the Wangyinpu Formation. The continuous thickness with greater than 50 ppm uranium is 27 m, from 2620 m to 2647 m. The total thickness with greater than 100 ppm uranium is 9 m, from 2620 m to 2690 m. The potential area of uranium resources in Xiuwu Basin is 840 km^2, and the geological uranium resources in Xiuwu Basin are calculated to be 4.9×10^3 t, which is a good prospect for uranium exploration.

4.4 Mode of enrichment of silicon and uranium in Wangyinpu shale

In the above discussion, the mechanism of silica and uranium enrichment in the Wangyinpu shale in the Xiuwu Basin is summarized, as shown in Figure 8. In the Early Cambrian period, due to the continuous activity of the super mantle plume, the Gondwana began to rift, and the Yangtze Plate and the Cathaysian Plate at the edge of the Gondwana underwent extension. The seawater was deep and highly reductive. Oceanic water penetrated into the deep seabed crust through the extensional faults between the two plates, and the infiltrated seawater was heated by magma and rose after substantial chemical exchange. Subsequently, the oceanic water escaped from the seabed in the form of submarine fountains. The hydrothermal fluids had temperatures as high as 75°C–102°C and were enriched in silicon and uranium. In addition, terrigenous detritus also carried some silicon and uranium, which were co-deposited from the two sources to form uranium-rich shale. Approximately 20%–40% of the silica in the shale came from seabed hydrothermal fluids, and the rest of it came from terrigenous debris; whereas more than 90% of the uranium element came from seabed hydrothermal fluids, and less than 10% came from terrigenous detritus.

5 Conclusions

1. In most parts of the Lower Cambrian Wangyinpu Formation shale in the Yangtze region, ~20%–40% of the silica in the shale was contributed by the hydrothermal fluids having temperatures of 75°C–102°C.
2. Sedimentary structures typically formed in the hydrothermal environment, such as scour surfaces, columnar structures, vein structures, contraction-like structures, horizontal laminated bed structures, and nodules were observed in the Wangyinpu For-

mation shale provide conclusive evidence for the wide spread hydrothermal activity in the studied area.

3. More than 90% of the uranium in most of the layers of the Lower Cambrian Wangyinpu Formation was derived from submarine hydrothermal fluids, while less than 10% was from terrigenous detritus.
4. Uranium was concentrated in the Middle-Upper part of the Lower Cambrian Wangyinpu Formation in the Xiuwu Basin. The geological uranium resources were 4.9×10^3 t, which was a good prospect for exploration. The uranium enrichment model for the uranium-rich shale in the Xiuwu Basin proposed here indicates extensional tectonics was responsible for the uranium enrichment through hydrothermal solutions.

Acknowledgement: This study was supported by the National Science and Technology Major Projects (No. 2017ZX05035-002), the Science Foundation of the Ministry of Land and Resources of China (No.12120114046701), the National Natural Science Foundation of China (No. 41472112 and No. 41728004) and open funds from the Sinopec Key Laboratory of Shale Oil/Gas Exploration and Production Technology. We sincerely appreciate all anonymous reviewers and the handling editor for their critical comments and constructive suggestions.

References

[1] Boyle, D.R., 1982. The information of basal-type urnium deposits in South Central Britishi Columbia. Economic Geology 77:1176–1209.

[2] Cawood, P.A., Memchin, A. A., Strachan, R., Prave, T., Krabbendam, M., 2007. Sedimentary basin and detrital zircon record along East Laurentia and Baltica during assembly and breakup of Rodinia. Journal of the Geological Society 164: 257–275.

[3] Cuney, M., Kyser, T.K., 2008. Recent and not-so-recent developments in uranium deposits and implications for exploration. Mineralogical Association of Canada, Short Course 39: 161–219.

[4] Cuney, M., 2010. Evolution of uranium fractionation process through time: Driving the secular variation of uranium deposit types. Economic Geology 105: 553–569.

[5] Holk, G.J., Kyser, T.K., Chipley, D., Hiatt, E.E., Marlatt, J., 2003. Mobile Pb-isotopes in Proterozoic sedimentary basins as guides for exploration of uranium deposits. Journal of Geochemical Exploration 80: 297–320.

[6] Islam, E., Paul, D., Sar, P., 2014. Microbial diversity in Uranium deposits from Jaduguda and Bagjata Uranium mines, India as revealed by Clone Library and Denaturing Gradient Gel Electrophoresis analyses. Geological biology Journal 2014: 3110.

[7] Leroy, J.L., George-Aniel, B., 1992. Volcanism and uranium mineralization: the concept of source rock and concentration mechanism. Journal of Volcanic Geothermal Research 50: 247–272. .

[8] Min, M., Luo, X., Du, G., He, B., Campbell, A.R., 1999. Mineralogical and geochemical constraints on the genesis of the granite-hosted Huangao uranium deposit, SE China. Ore Geol. Rev. 14(2): 105–127.

[9] Min, M., Xu, H., Chen, J., Fayek, M., 2005. Evidence of uranium biomineralization in sandstone-hosted roll-front uranium deposits, Northwestern China. Ore Geology Reviews 26: 198–206.

[10] Martin-Izard, A., Arribas, A., Sr Arias, D., Ruiz, J., Fernandez, F.J., 2002. The Fe deposit, West-Central Spain; tectonic-hydrothermal uranium mineralization associated with transpressional faulting of Alpine age. Canadian Mineralogy 40: 1505–1520.

[11] Wang, Y., Hu, B., Gao, H., Li, W., Bai, H., Guo, G., 2014. Existing and enriching mechanism of uranium minerals from Lower Cambrian black rock series in Xiuwu Basin. Uranium Geology 30 (1): 1–6 (in Chinese with English abstract).

[12] Zhang, W., Li, Z., 2005. Metallogenetic characteristics and material source of Zoujiashan uranium deposit, Jiangxi Province. Geoscience 19 (3): 369–374 (in Chinese with English abstract).

[13] Qi, F., Li, Z., Wang, W., Yang, Z., Peng, B., Wang, Z., Dong, Y., 2016. Discovery and geological significance of nanoscale brannerite from marine phosphorite in the Northwestern Hunan. Journal of Earth Sciences and Environment 38 (5): 569–577 (in Chinese with English abstract).

[14] Bishop, J.K.B., 1988. The barite-opal-organic carbon association in oceanic particulate matter. Nature 332(24): 341–343.

[15] Torres, M.E., Brumsack, H.J., Bohrmann, G., Emeis, K.C., 1996. Barite fronts in continental margin sediments: A new look at barium remobilization in the zone of sulfate of sulfate reduction and formation of heavy barites in diagenetic fronts. Chem. Geol. 127, 125–139.

[16] Aquilina, L., Dia, A.N., Boulegue, J., Fouillac, A.M., 1997. Barite deposits in Covergent margin off Peru: Implications for fluid circulation within subduction zones. Geochim. Cosmochim. Acta 61(6): 1233–1245.

[17] Yang, R., Wei, H., Bao, M., Wang, W., Wang, Q., 2007. Submarine Hydrothermal Venting —Flowing Sedimentary Characters of the Cambrian Shanggongtang and Dahebian Barite Deposits, Tianzhu County, Guizhou Province. Geological Review 53(5): 675–680 (in Chinese with English abstract).

[18] Holdaway, H.K., Clayton, C.J., 1982. Preservation of shell microstructure in silicified brachiopods from the upper cretaceous Wilmington sands of Devon. Geol. Mag.119, 371–382.

[19] Wedepohl, K.H., 1971. Environmental influences on the chemical composition of shales and clays. Phys. Chem. Earth 8, 307–331.

[20] Adachi, M., Yamamoto, K., Sugisaki, R., 1986. Hydrothermal chert and associated siliceous rocks from the Northern Pacific: their geological significance as indication of ocean ridge activity. Sediment. Geol. 47 (1), 125–148.

[21] Yamamoto, K., 1987. Geochimical characteristics and depositional environments of cherts and associated rocks in the Franciscan and Shimanto terrenes. Sediment. Geol. 52, 65–108.

[22] Bostrom, K., Kraemer, T., Gratner, S., 1973. Provenance and accumulation rates of opaline silica, Al, Ti, Fe, Mn, Cu, Ni, and Co in Pacific pelagic sediments. Chem. Geol. 11(2):123–148

[23] Douthitt, C.B., 1982. The geochemistry of the stable isotopes of silicon, Geoch. Cosmoch. Acta 46(8): 1449–1458.

[24] Savin, S.M., Epstein, S., 1970. The oxygen isotopic compositions of coarse grained sedimentary rocks and minerals. Geoch. Cos-

moch. Acta 34 (3): 323–329.
[25] Knauth, P.L., Epstein, S., 1976. Hydrogen and oxygen isotope rations in nodular and bedded cherts. Geoch. Cosmoch. Acta 40(9): 1095–1108.
[26] Taylor, S.R., McLennan, S.M., 1985. The Continental Crust; Its composition and evolution; an examination of the geochemical record preserved in sedimentary rocks. Blackwell, Oxford. 312.
[27] Algeo, T.J., Kuwahara, K., Sano, H., Bates, S., Lyons, T., Elswick, E., Hinnov, L., Ellwood, B., Moser, J., Maynard, B.J., 2011. Spatial variation in sediment fluxes, redox conditions, and productivity in the Permian-Triassic Panthalassic Ocean. Palaeogeogr. Palaeocl. 308 (1), 65–83.
[28] Zhu, M., Zhang, J., Yang, A., Li, G., Steiner, M., Erdtmann, B.D., 2003. Sinian-Cambrian stratigraphic framework for shallow-to deep-water environments of the Yangtze Platform: An integrated approach. Prog. Nat. Sci. 13(12): 951–960
[29] Zhu, M., Babcock, L.E., Peng, S., 2006. Advances in Cambrian stratigraphy and paleontology: Integrating correlation techniques, paleobiology, taphonomy and paleoenvironmental reconstruction. Palaeoworld 15(3/4): 217–222.
[30] Xiao, K., Chen, H., Wo, Y., Zhou, Y., Zhang, Y., 2005. Impact of tectonic evolution on Paleozoic and Mesozoic petroleum systems in Jianghan plain. Oil Gas Geol. 26 (5), 688–693 (in Chinese with English abstract).
[31] Guo, F., Kang, J., Sun, J., Lu, J., Wang, X., 2010. Tectonic evolution and hydrocarbon accumulation model for marine strata in Jianghan Basin. Lithol. Reserv. 22 (1): 23–29 (in Chinese with English abstract).
[32] Feng, Z., Peng, Y., Jin, Z., Jiang, P., Bao, Z., Luo, Z., Ju, T., Tian, H., 2001. Lithofacies paleogeography of the Cambrian in South China. J. Paleogeogr. 3 (1): 1–14 (in Chinese with English abstract).
[33] Yang, J., Yi, F., Hou, L., 2004. Genesis and petrogeochemistry characteristics of Lower Cambrian black shale series in Northern Guizhou. Acta Miner. Sin. 24 (3): 286–291 (in Chinese with English abstract).
[34] Qi, X., Hu, Q., Yi, X., Zhang, S., 2015. Shale gas exploration prospect of lower Cambrian Wangyinpu Formation in Xiuwu Basin. China Min. Mag. 24 (10): 102–107 (in Chinese with English abstract).
[35] Wang, G., Ju, Y., Han, K., 2015. Early paleozoic shale properties and gas potential evaluation in Xiuwu Basin, western lower Yangtze Platform. J. Nat. Gas. Sci. Eng. 22: 489–497.
[36] Mei, L., Deng, D., Shen, C., Liu, Z., 2012. Tectonic dynamics and marine hydrocarbon accumulation of Jiangnan-Xuefeng Uplift. Geol. Sci. Technol. Inf. 31 (5): 85–93 (in Chinese with English abstract).
[37] Zhang, K., Jiang, Z., Xie, X., Gao, Z., Liu, T., Yin, L., Jia, C., Song, Y., Shan, C., Wu, Y., Wang, P., 2018. Lateral Percolation and Its Effect on Shale Gas Accumulation on the Basis of Complex Tectonic Background. Geofluids 2018, doi: 10.1155/2018/5195469
[38] Jiang, Y., Li, S., 2005. A study of the fluid environment of silicalite of transitional Precambrian-Cambrian age in Hunan and Guizhou provinces. Earth Science Frontiers 12(4): 622–629 (in Chinese with English abstract).
[39] Murray, R.W., Buchholtz, T. B. M. R., Gerlach, D.C., 1991. Rare earth, major, and trace elements in chert form the Franciscan complex and monterey group, California: assessing REE sources to fine-grained marine sediments. Geochim. Cosmochim. Ac. 55(7):1875–1895.
[40] Liu, J., Zheng, M., 1993. Geochemistry of hydrothermal sedimentary silicalite. Acta Geological Sichuan 13(2):110–118 (in Chinese with English abstract).
[41] Yang, J., Wang, D., Mao, J., Zhang, Z., Zhang, Z., Wang, Z., 1999. The petrochemical research method for silicalite and its application to the "Jingtieshan Type" iron deposits. Acta Petrologica et Mineralogical 18(2): 108–118 (in Chinese with English abstract).
[42] Liu, J., Li, Y., Zhang, Y., Liu, S., Cai, Y., 2017. Evidences of biogenic silica of Wufeng-Longmaxi Formation shale in Jiaoshiba area and its geological significance. Journal of China University of Petroleum (Edition of Natural Science) 41(1):34–41(in Chinese with English abstract).
[43] Jiang, S., Palmer, M.R., Ding, T., Wan, D., 1994. Silicon isotope geochemistry of the Sullivan Pb-Zn deposit, Canada: A preliminary study. Economic Geology and the Bulletin of the Society of Economic Geologists 89: 1623–1639.
[44] Hearing, T.W., Harvey, T.H.P., Williams, M., Leng, M.J., Lamb, A.L., Wilby, P.R., Gabbott, S.E., Pohl, A., Donnadieu, Y., 2018. An early Cambrian greenhouse climate. Science advances 4(5): eaar5690.
[45] Zhang, K., Jiang, Z., Yin, L., Gao, Z., Wang, P., Song, Y., Jia, C., Liu, W., Liu, T., Xie, X., Li, Y., 2017. Controlling functions of hydrothermal activity to shale gas content-taking lower Cambrian in Xiuwu Basin as an example. Mar. Pet. Geol. 85 (2017), 177–193.
[46] Zhang, K., Li, Z., Jiang, S., Jiang, Z., Wen, M., Jia, C., Song, Y., Liu, W., Huang, Y., Xie, X., Liu, T., Wang, P., Shan, C., Wu, L., 2018. Comparative Analysis of the Siliceous Source and Organic Matter Enrichment Mechanism of the Upper Ordovician–Lower Silurian Shale in the Upper-Lower Yangtze Area. Minerals 2018(8), doi:10.3390/min8070283
[47] Zhang, K., Song, Y., Jiang, S., Jiang, Z., Jia, C., Huang, Y., Liu, X., Wen, M., Wang, X., Li, X., Wang, P., Shan, C., Liu, T., Liu, W., Xie, X., 2019. Shale gas accumulation mechanism in a syncline setting based on multiple geological factors: An example of southern Sichuan and the Xiuwu Basin in the Yangtze Region. Fuel 241 (2019), 468–476.
[48] Zhang, K., Song, Y., Jiang, S., Jiang, Z., Jia, C., Huang, Y., Wen, M., Liu, W., Xie, X., Liu, T., Wang, P., Shan, C., Wu, Y., 2019. Mechanism analysis of organic matter enrichment in different sedimentary backgrounds: A case study of the Lower Cambrian and the Upper Ordovician-Lower Silurian, in Yangtze region. Mar. Petrol. Geol.99, 488–497.
[49] Korzhinsky, M.A., Tkachenko, S.I., Shmlovich, K.I., 1994. Discovery of a pure rhenium mineral at Kudriavy volcano. Nature 369, 51–52.